XIII International Conference on Computational Plasticity. Fundamentals and Applications
COMPLAS XIII
E. Oñate, D.R.J. Owen, D. Peric and M. Chiumenti (Eds)

FE SIMULATION OF THE EXPANSION OF A WE43 MAGNESIUM ALLOY STENT IN A REPRESENTATIVE BLOOD VESSEL

SHOICHIRO YOSHIHARA [*], GO IWAMATSU [*], YOSHIHIRO AMIKURA [*] AND BRYAN J. MACDONALD[†]

[*] Department of Mechanical System Engineering,
University of Yamanashi
4-3-11 Takeda, Yamanashi 400-8511, Japan
e-mail: yoshihara@yamanashi.ac.jp, www. yamanashi.ac.jp

[†] School of Manufacturing and Mechanical Engineering
Dublin City University DCU
Collins Avenue, Dublin 9, Ireland
e-mail: bryan.macdonald@dcu.ie, www.dcu.ie

Key words: Plasticity, Forming Process, WE43 Magnesium Alloy Stent, FE Simulation.

Abstract. Magnesium alloys have been expected as bio-materials such as a stent for a blood vessel and a screw bolt for joining bones and so forth. Expansion deformation behavior of WE43 magnesium alloy, which have been adopted as the bio-mechanics for the stent, were examined for the optimum design of the stent without any fracture in FE simulation. In this study, we have evaluated stress and strain on the difference width and thickness of the stent in FE simulation. Furthermore, WE43 magnesium alloy stent was expanded in the experiment in order to evaluate the expanded shape in comparison with FE simulation result. The thickness and the width of the stent should be considered for the optimum design.

1 INTRODUCTION

In recent years, there has been growing interest in the application of magnesium alloy materials to the manufacture of cardiovascular stents which are used to expand blood vessels which have narrowed due to disease [1]. Conventional permanent stents, manufactured from stainless steel or titanium alloys, have seen widespread use but have recently been recognized as being limited by stent thrombosis and in-stent restenosis. Magnesium alloy stents, which naturally corrode and are absorbed in the body over time, have the potential to overcome many of the problems associated with conventional stent technology [2]. It is imperative, however, to fully understand the material deformation behavior during the deployment of magnesium alloy stents in order to avoid problems such as material fracture during the expansion process. There are currently very few studies on the deformation mechanisms of magnesium alloy tubes and stents. It is particularly important to accurately predict fracture during the expansion process as there is significant potential to damage to the blood vessel

and cause increased patient suffering. Thus, in this study, the material fracture of magnesium alloy stents has been evaluated and predicted using a combination of finite element analysis (FEA) and a ductile fracture criterion. Furthermore, the effect of the thickness and the width of the stent on stress and strain were studied for the optimal shape of the stent. Besides, the ductile fracture criterion is then used to predict failure of a magnesium alloy stent when deployed in a representative diseased blood vessel.

2 FE SIMULATION CONDITIONS

2.1 Stent model

Figure 1 shows the stent model using FE simulation. Actual two types of stent model were defined in this study in order to confirm the difference deformation of the materials during the expansion process. The model in FE simulation was consist of the stent , the plaque , the balloon and the artery as shown in Figure 2.

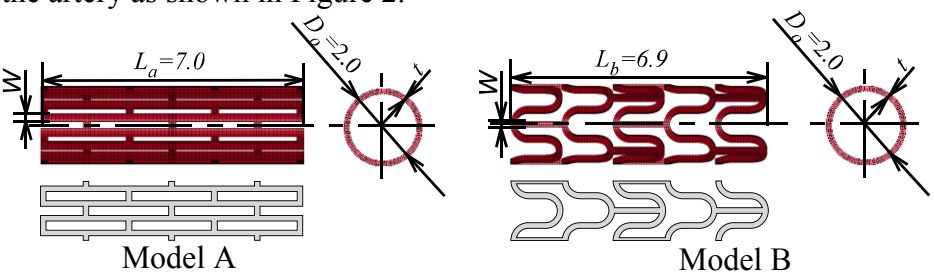

Figure 1: Stent model and quarter expansion plan

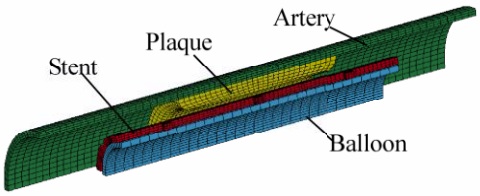

Figure 2: FEA model of expanding of Artery by stent

2.2 Material properties

The FEA code ANSYS/LS-DYNA3D was used. Figure 3 shows the stress-strain curve of WE43 magnesium alloy tube which would be expected as the medical device for our body in recent years. Also, Table 1 shows the material properties of the WE43 magnesium alloy tubes. An elasto-plastic material was assumed, satisfying the n-power law with the constitutive equation,

$$\sigma = C\varepsilon^n \tag{1}$$

where, C is the plastic modulus, ε the strain and n the work-hardening exponent. These parameters were used in FE simulation. Furthermore, the characteristics of the balloon, the artery and the plaque were indicated in Table 2. The solid element was utilized in the stent, the baloon, the artery and the plaque.

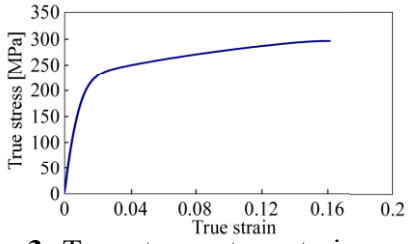

Figure 3: True stress - true strain curve

Table 1: Material properties of workpiece

Modulus of elasticity E[GPa]	20.1
*F value [MPa]	383
*n value	0.14
Tensile strength σ[MPa]	252

Table 2: Material properties of balloon, artery and plaque

	Balloon	Artery	Plaque
Density $\rho\times10^{-6}$[kg/mm^3]	1.07	1.07	1.07
Modulus of elasticity E [MPa]	———	1.75	2.19
Poisson's ratio υ	0.495	0.499	0.499

2.3 Simulation conditions

Table3 shows the FE simulation conditions in expansion of the stent. The thickness of the stent was set on 0.10, 0.15 and 0.20mm and the width 0.10, 0.15 and 0.20mm in this study. Figure 4 shows the relationship between the inner pressure of the balloon and solution time. The inner pressure was linearly increased during the initial stage (0-0.8s). P_{max} has been defined as the maximum pressure when the inner diameter at the plaque would be 3.0mm. Figure 5 shows the images of the expanded stent in FE simulation. The friction coefficient between the stent and the balloon was set on 0.1. Also, the friction coefficient between the stent and the plaque, the plaque and the artery was respectively set on 0.1.

Table 3: FE simulation conditions of expanding stent model

(a) Model A

CASE	Thickness t [mm]	Width of frame W [mm]	Element	Node
AI	0.15	0.15	3852	6688
AII	0.10	0.15	2592	5055
AIII	0.20	0.15	5136	8355
AIV	0.15	0.10	2610	4984
AV	0.15	0.20	5124	8372

(b) Model B

CASE	Thickness t [mm]	Width of frame W [mm]	Element	Node
BI	0.15	0.15	4110	7364
BII	0.10	0.15	2740	5514
BIII	0.20	0.15	5736	9585
BIV	0.15	0.10	2580	5324
BV	0.15	0.20	5252	8772

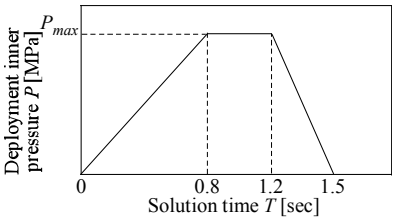

Figure 4: Load curve of inner pressure

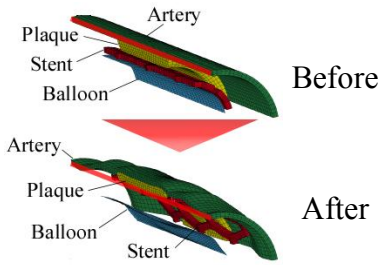

Figure 5 :FEA model before and after expanding

3 FE RESULTS

3.1 Effect of difference thickness of stent

Figure 6 shows the relationship between the minimum inner diameter at the plaque and the inner pressure on the different thickness of the stent. The minimum inner diameter was increased in both models as the inner pressure was increased as shown in Figure 6. For example, the minimum inner diameter in CASE [AIII] was 3.5mm and CASE [BIII] 3.05mm at the inner pressure 2MPa. Therefore it is ease to deform the stent Model A more than Model B. Besides, it is difficult to expand the stent as the thickness of the stent was increased in both cases. Moreover, it is confirmed that the inner diameter bears a direct relation to the inner pressure as shown in Figure 6.

Figure 7 shows Von Mises stress and plastic strain distribution of the expanded stent at the inner diameter 3.0mm. In both cases, stress and strain were increased as the thickness of the stent was decreased. Stress and strain in Model A are high owing to the tension stress by bending as shown in Figure 7(a). On the contrary, these parameters are high at the T part of the stent. Thickness of the stent in Model B has been had high impact on stress and strain more than Model A.

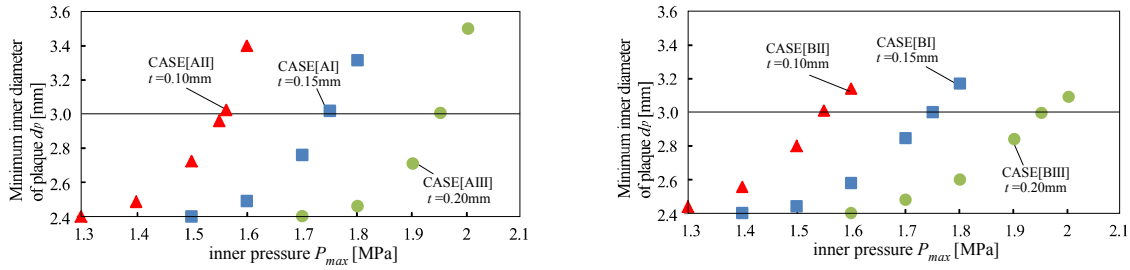

(a) Model A **(b)** Model B

Figure 6: Relationship between minimum inner diameter of plaque and maximum inner pressure

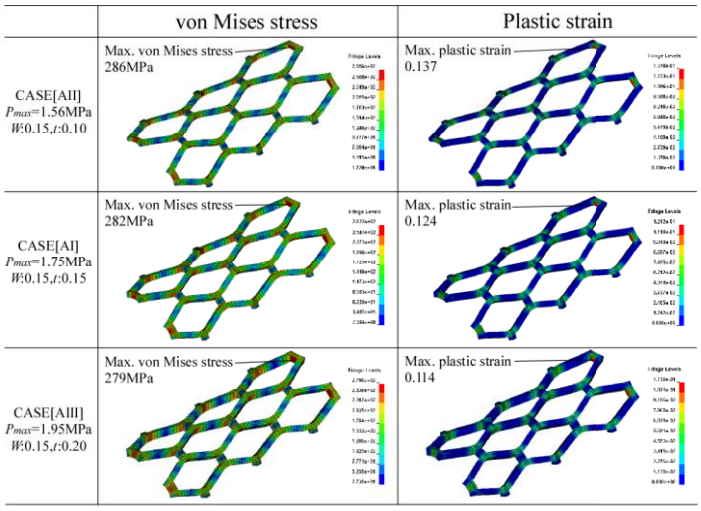

(a) Model A

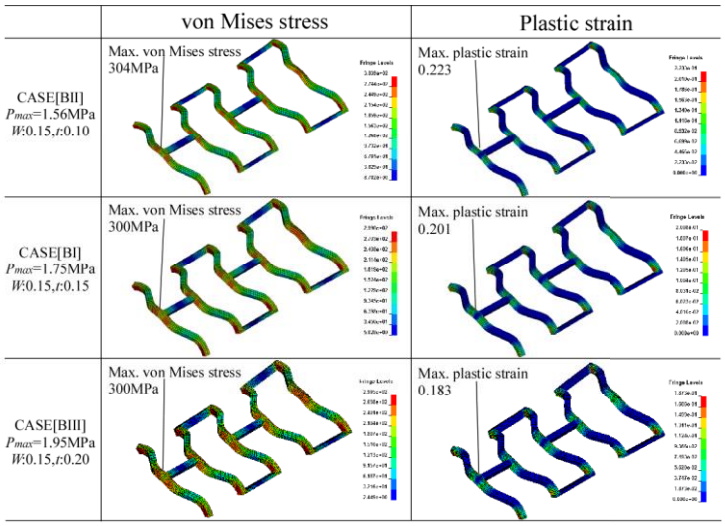

(b) Model B

Figure 7: Von Mises stress and plastic strain distribution of stent

3.2 Effect of difference width of stent

Figure 8 shows the relationship between the minimum inner diameter at the plaque and the inner pressure on the different width of the stent. It is easy to deform the stent of Model B more than Model A because it is impossible to expand the inner diameter 3.0mm in CASE [AIV]. Figure 9 shows Von Mises stress and plastic strain distribution of the expanded stent at the inner diameter 3.0mm without CASE [AIV]. Stress in case of Model B is slightly high in comparison with Model A. Stress and strain on the stent are increased as the width is increased because of the effect of the plane bending.

4 COMPARISON BETWEEN FE SIMURATION AND EXPERIMENT

4.1 Experimental conditions

Figure 10 shows the photo of WE43 magnesium alloy stent and FE simulation model, Figure 11 the photo of the experimental tool for expanding the WE43 magnesium alloy stent. The experimental tool consists of the pressurizer, the balloon, the syringe and the valve. The balloon is inserted in the stent before the stent would be expanded as shown in Figure 11.

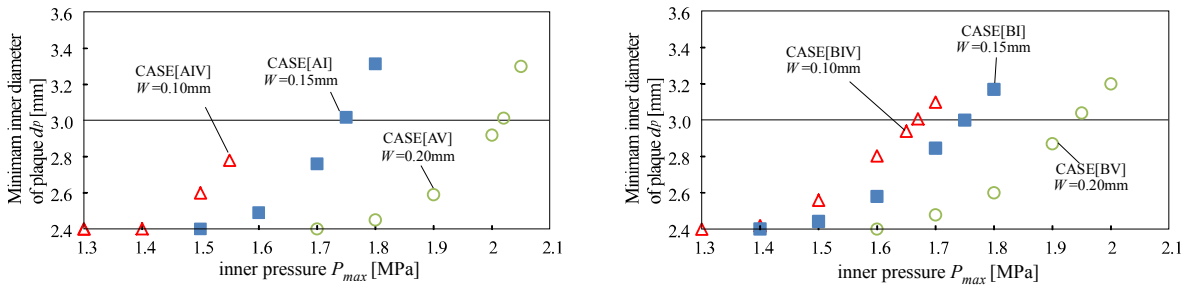

(a) Model A **(b)** Model B

Figure 8: Relationship between minimum inner diameter of plaque and maximum inner pressure

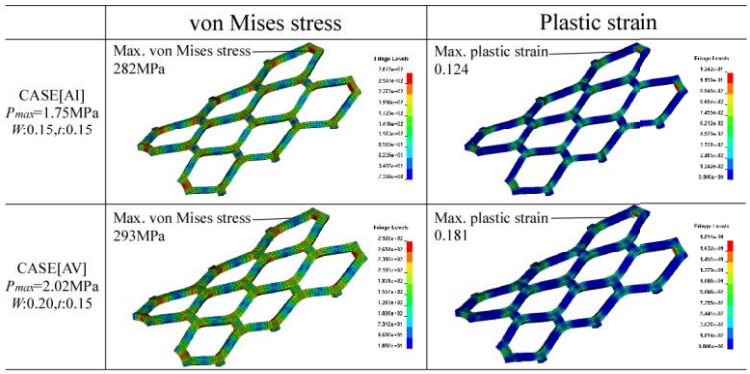

(a) Model A

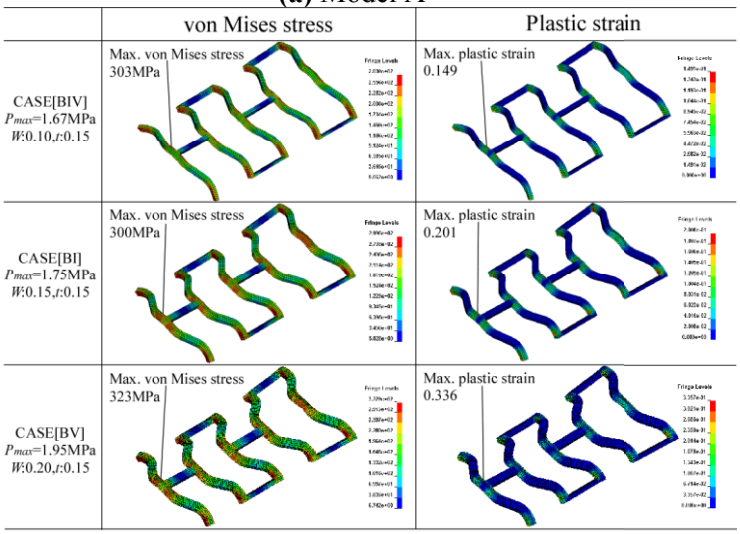

(b) Model B

Figure 9: Von Mises stress and Plastic strain distribution of stent

Figure 10: Photograph of WE43 magnesium alloy stent and FEA model

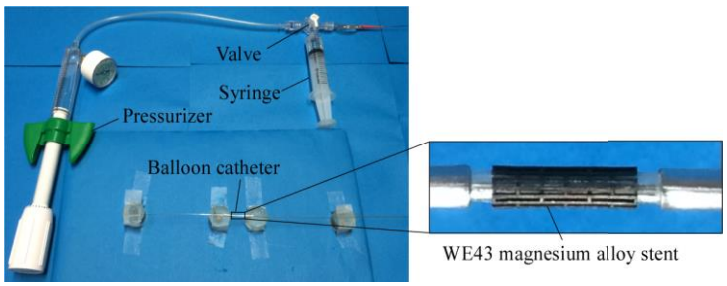

Figure 11: Photograph of experimental

4.2 Comparison with between FE simulations and experiment

Figure 12 shows the photo and FE simulation results of the stent after expansion deformation. In the experiment, the maximum pressure at the fracture of the stent was 0.7MPa. On the other hand, the pressure at the fracture in FE simulation was 2.0MPa by using ductile fracture criterion as the fracture evaluation [3]. The difference of the fracture pressure between the experiment and FE simulation was not small as the surface roughness of the stent manufactured by laser forming is not small. However, the expanded shape of the stent in the experiment is according to the result of FE simulation as shown in Figure 12.

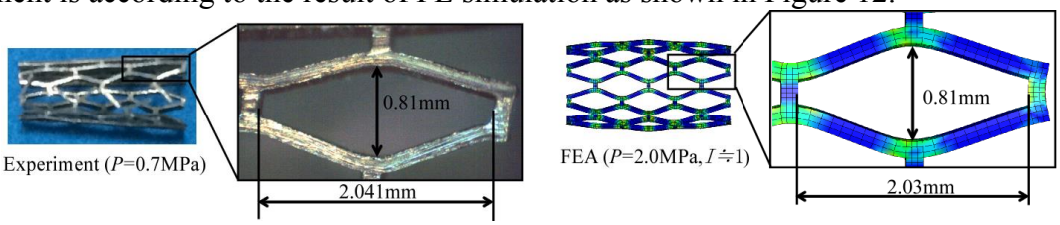

Figure 12: Experiment and FEA result of deformation of stent in CASE2

5 CONCLUSIONS

- It was confirmed that the width and the thickness of the stent have influenced the stress and strain distribution after the process from the results of FE simulation. Especially, stress was increased as the width of the stent was increased. Therefore, the stent model, the thickness and the width should be considered for the optimal shape.
- The expanded shape of the stent in the experiment is according to the result of FE simulation. Thus, the deformed shape and the fracture point after the process might be predicted by FE simulation.

REFERENCES

[1] http://www.nims.go.jp/jpn/news/press/pdf/press136.pdf , (2006)(in Japanese).
[2] E. Galvin, M. M. Morshed, C. Cummins, S. Daniels, C. Lally and B. MacDonald, “Surface Modification of Absorbable Magnesium Stents by Reactive Ion Etching”, Plasma Chem Plasma Process, **33**, 1137–1152 (2013).
[3] H. Takuda, T. Kanie, E. Isogai and T. Yoshida, “Finite Element Analysis of Forming Limit of High-Strength Steels Using Ductile Fracture Criterion”, ISIJ, **91**, 43-49(2005) (in Japanese)